Microscopic muon dynamics in the polymer electrolyte poly(ethylene oxide)

Iain McKenzie[1,2,*] and Stephen P. Cottrell[3]
[1]*TRIUMF, Vancouver, B.C., Canada, V6T 2A3*
[2]*Department of Chemistry, Simon Fraser University, Burnaby, B.C. Canada, V5A 1S6*
[3]*ISIS, Rutherford Appleton Laboratory, Chilton, Didcot, Oxon, OX11 0QX, United Kingdom*
(Received 2 February 2017; published 18 July 2017)

The microscopic dynamics of protons (H^+) in poly(ethylene oxide) (PEO) have been investigated through a study of implanted positive muons (Mu^+), which can be considered a light proton analog. The exponential decay of the muon spin polarization in zero magnetic field indicated that Mu^+ hopping is in the fast fluctuation limit between 140 and 310 K and the relaxation rate was found to be sensitive to the glass transition. Mu^+ dynamics in PEO was monitored via the relaxation of the muon spin polarization in a transverse field of 10 mT. Activated hopping of Mu^+ was observed above the glass transition temperature with an activation barrier of 122 ± 1 meV. The temperature dependence of the diamagnetic muon polarization in PEO can be explained by diffusion of radiolytic electrons.

DOI: 10.1103/PhysRevE.96.012502

I. INTRODUCTION

Solid polymer electrolytes (SPE) have attracted widespread interest because of their potential applications in solid electrochemical devices such as energy conversion units (batteries or fuel cells), electrochromic display devices or smart windows and sensors [1]. SPEs offer advantages over traditional ceramic and commercial liquid electrolytes in that they are flexible and moldable and avoid the use of volatile solvents [2]. Proton-(H^+) based rechargeable batteries could be an alternative to a lithium-ion-based system because of the availability of low-cost proton conductors, especially for low-energy-density applications [3]. SPEs are also a key component of polymer electrolyte membrane fuel cells [4].

Poly(ethylene oxide) (PEO) is one of the most widely used SPEs due to its low glass transition temperature ($T_g \sim 215$ K) and ability to dissolve high concentrations of ionic species. Proton conducting membranes and electrochromic devices have been produced using PEO [5–7]. The dc conductivity of molten 20 kg mol^{-1} PEO at 373 K is 2.5×10^{-7} S cm^{-1} and the activation energy is 235 meV [8]. The conductivity of PEO increases to $\sim 10^{-5}$ S cm^{-1} with the inclusion of salts such as NH_4ClO_4 [5] and NH_4I [6]. Understanding the microscopic dynamics of protons embedded in a polymer matrix is crucial for interpreting ionic transport and optimizing SPE for battery and fuel cell applications. There have been few studies of microscopic proton dynamics in PEO. Donoso *et al.* used nuclear magnetic resonance (NMR), impedance spectroscopy, and neutron scattering to examine PEO with high concentrations of H_3PO_4 (H_3PO_4/EO=0.42 and 0.66) [9]. The conductivity was found to be driven by the segmental motion of the PEO chains and the temperature dependence in the less-concentrated sample was well described by the Vogel-Fulcher-Tammann equation [10]. The NMR measurements showed the correlation time of the acidic proton in deuterated PEO decreases by approximately four orders of magnitude from 263 to 322 K.

We have investigated proton diffusion in PEO by using the positive muon (Mu^+), which is considered to behave like a light proton in condensed matter, as a radioactive tracer for the proton [11]. Information about the local environment of the muon and its dynamics can be obtained from a collection of magnetic resonance techniques known as muon spin rotation, relaxation and resonance (μSR) [12,13]. Muons (lifetime ~ 2.2 μs) are produced and implanted with 100% spin polarization, enabling measurements to be carried out with great sensitivity, particularly when compared to conventional magnetic resonance methods. The positive muon decays to a positron and two neutrinos, with the positron emitted preferentially along the direction of the muon's spin; thus the detection of decay positrons in a given direction provides a convenient means of monitoring the spin polarization of an ensemble of muons. Spectra were obtained in zero field (ZF) and in transverse fields (TF). The measurements reported in this paper are closely analogous to those of T_1 (spin-lattice relaxation) and T_2 (spin-spin relaxation) that are familiar in conventional magnetic resonance. The precession in TF is analogous to the free induction decay in NMR.

In nonmetallic samples, implanted muons thermalize into both diamagnetic and paramagnetic states. The paramagnetic state in PEO is muonium (Mu), which can be considered a light isotope of hydrogen. It is the diamagnetic muons that provide an ideal mimic for proton mobility, although one must consider the lower mass of the muon at low temperatures where quantum tunneling between lattice sites is important [11]. The light mass of the muon should also result in larger attempt frequencies but the energetic barriers should be independent of the mass at the temperatures considered in the experiments described herein. It is not possible to determine the local chemical environment of diamagnetic muons from spectroscopic measurements at present because typical chemical shift values are smaller than the uncertainty in the precession frequency due to the short lifetime of the muon. μSR has been used to study Mu^+ diffusion in a range of materials such as the inorganic proton conductor $Zr(H_2PO_4)(PO_4) \cdot 2H_2O$ [14] and metals such as Cu [15]. It has also been used to study dynamics in polymers such as PTFE [16,17]. The μSR measurements are used to study dynamics

*iain.mckenzie@triumf.ca

in an essentially pure PEO sample since there are only at most a few hundred muons in the sample at any one time.

II. EXPERIMENTAL

PEO was purchased from Sigma-Aldrich and had a molecular weight of 5×10^6 g mol^{-1}. The bulk glass transition temperature (T_g) was determined to be 213 K and the degree of crystallization is estimated to be 65 % from differential scanning calorimetry measurements. PEO was dehydrated following the procedure of Mattsson *et al.* [18] and ~2 g was loaded into the recessed cavity (28.5 mm diameter and 1.5 mm deep) of an aluminium sample holder in a glovebox with a dry environment. The PEO powder was covered with a 100-μm-thick titanium foil window with an indium seal. A high purity silver mask was mounted on the front of the holder to intercept beam not stopped in the sample.

The μSR measurements were performed at the ISIS pulsed neutron and muon facility in Chilton, Didcot, Oxfordshire, U.K., using the EMU spectrometer [19]. The sample was mounted on a closed cycle refrigerator which controlled the temperature to $\pm$0.1 K. Transverse-field muon spin rotation (TF-μSR) measurements were made in a magnetic field of 10 mT as a function of temperature cooling from 310 to 145 K. Zero-field muon spin relaxation (ZF-μSR) measurements were made on heating the sample from 145 K. The polarization (P) is proportional to the asymmetry (A) in the decay positrons counted in the forwards and backwards directions with respect to the initial muon polarization. P is given by A/A_0, where A_0 is the full asymmetry of the spectrometer (21.5%) and was determined from TF measurements in silver (where all of the muons are in a diamagnetic environment).

Density functional theory (DFT) calculations were performed with the Gaussian 09 package of programs [20]. The calculations used the unrestricted B3LYP functional and the DGDZVP basis set.

III. RESULTS AND DISCUSSION

A. ZF-μSR measurements of dynamics in PEO

ZF-μSR measurements have been used to study the dynamics of Mu^+ [14] and other ions such as Li^+ in a wide range of materials [21–23]. The motion of the ions results in a fluctuating local magnetic field at the muon, which is due to the dipolar fields of randomly oriented nuclear moments surrounding the muon, such as protons. The fluctuating local magnetic field causes the muon spin polarization to relax. If there is a Gaussian distribution of local fields with width Δ/γ_μ, where γ_μ is the muon gyromagnetic ratio, the time dependence of the muon spin polarization is given by the Kubo-Toyabe (KT) function:

$$P_z(t) = \tfrac{1}{3} + \tfrac{2}{3}\left(1 - \gamma_\mu^2\Delta^2 t^2\right)e^{-\frac{1}{2}\gamma_\mu^2\Delta^2 t^2}. \quad (1)$$

The KT relaxation function looks like a Gaussian function at early times, goes to a minimum at $t = \sqrt{3}/\Delta$, and has a $\frac{1}{3}$ tail at long times. Fluctuations of the local field, with a correlation time τ, will affect the relaxation function. When the fluctuation rate is small (i.e., $\tau^{-1} < 0.5\gamma_\mu\Delta$), the main effect is a relaxation of the $\frac{1}{3}$ tail. In the case of fast fluctuations (i.e., $\tau^{-1} \geqslant \gamma_\mu\Delta$), one observes an exponential decay of the polarization with a decay constant, λ, given by [12]:

$$\lambda = 2\gamma_\mu^2\Delta^2\tau. \quad (2)$$

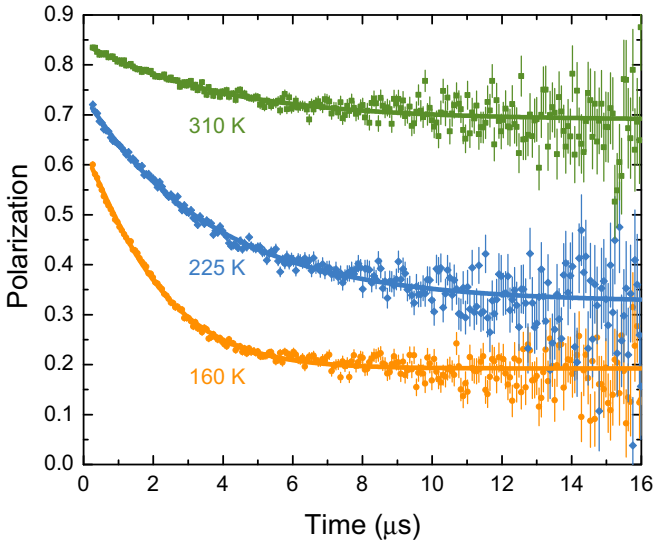

FIG. 1. ZF-μSR spectra of PEO at 160, 225, and 310 K. The solid lines are fits to Eq. (3).

ZF-μSR spectra of PEO at 160, 225, and 310 K are shown in Fig. 1. The spectra were well described by the following model:

$$P(t) = P_R e^{-\lambda t} + P_{NR}, \quad (3)$$

where P_R is the relaxing polarization, P_{NR} is the nonrelaxing polarization, and λ is the relaxation rate. No recovery of spin polarization was observed at long times. The exponential decay of the muon spin polarization in ZF indicates that the system is in the motional narrowing limit at all of the temperatures studied, which means $\tau^{-1} \gg \gamma_\mu\Delta$. Δ can be calculated using the van Vleck formula [12,24]:

$$\Delta^2 = \frac{2}{3}\left(\frac{\mu_0}{4\pi}\right)^2\gamma_I^2\hbar^2 I(I+1)\sum_j r_j^{-6}, \quad (4)$$

where γ_I is the gyromagnetic ratio of the nuclear spin, I, and r_j is the distance between the nuclear spin j and the muon. DFT calculations were performed for a small fragment of PEO with Mu^+ bound to the oxygen and we estimate that $\gamma_\mu\Delta \sim 1.6 \times 10^6$ rad s^{-1}. This is a lower limit for $\gamma_\mu\Delta$ as we have ignored contributions from neighboring PEO chains. The ZF-μSR measurements indicate that τ must be much less than ~625 ns rad^{-1} at even the lowest temperature studied.

A comparison between the polarization measured in the TF (see next section) and ZF measurements at the same temperature suggests there is a sizable component in the ZF signal due to T_1 relaxation of Mu (Fig. 2). It is not possible to disentangle the relaxation of the diamagnetic and paramagnetic components in PEO. There is a noticeable change in the values of P_R and P_{NR} at T_g; these components appear to trade off with respect to each other, with the total polarization in ZF increasing monotonically.

λ changes substantially with temperature (Fig. 3). The decrease of λ with increasing temperature below T_g can be understood in terms of Eq. (2); τ decreases with increasing

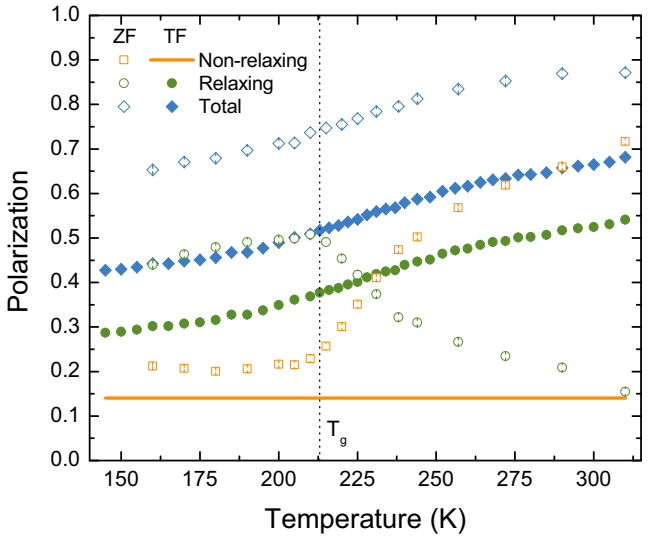

FIG. 2. Temperature dependence of the polarizations of the relaxing and nonrelaxing signals obtained from the the ZF-μSR [Eq. (3)] and TF-μSR spectra [Eq. (5)].

temperature. λ has a minimum value at T_g, so ZF-μSR can be used to determine T_g in PEO. It is not clear why there is a minimum in λ at T_g but it is most likely due to the spin relaxation involving both Mu^+ and Mu as described above. This inability to deconvolute the contributions from Mu^+ and Mu means that despite ZF-μSR generally being the more sensitive method for studying diffusion processes, it is not the best tool to study fast Mu^+ dynamics in PEO.

B. TF-μSR measurements of Mu^+ dynamics in PEO

TF-μSR spectra of PEO in a transverse field of 10 mT at 160 and 310 K are shown in Fig. 4. The TF-μSR spectra were fit with two oscillating components,

$$P(t) = P_D \cos(\omega_L t + \phi) e^{-t/T_2^\mu} + P_{Bg} \cos(\omega_L t + \phi), \quad (5)$$

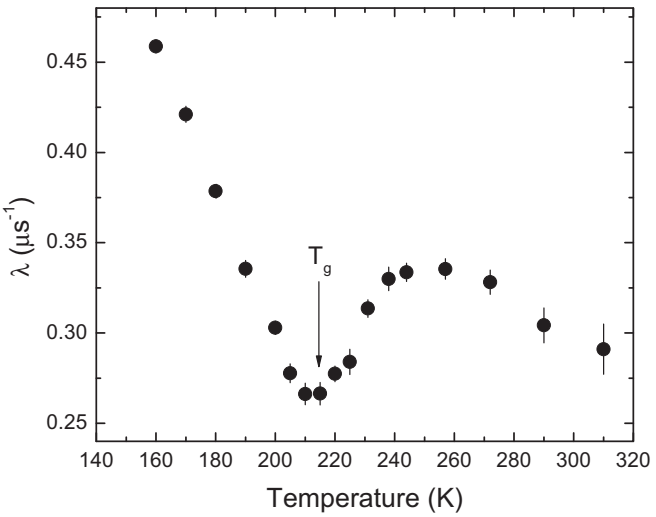

FIG. 3. Temperature dependence of the zero-field spin relaxation rate in PEO obtained from Eq. (3).

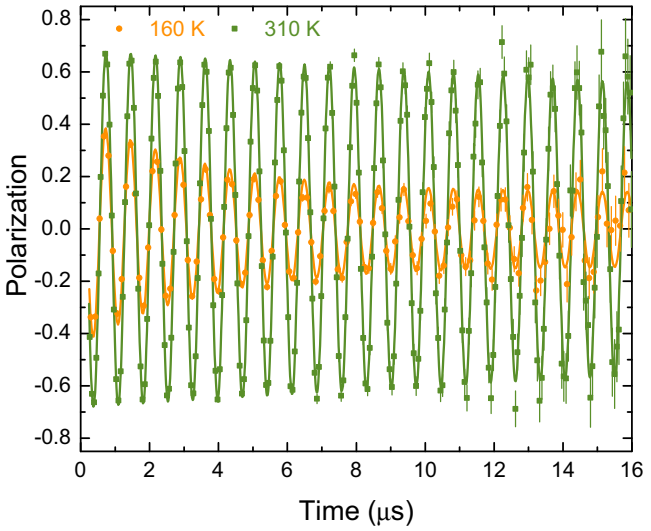

FIG. 4. TF-μSR spectra of PEO in an applied field of 10 mT at 160 and 310 K. The solid lines are fits to Eq. (5).

where P_D is the polarization due to diamagnetic muons stopped in PEO, P_{Bg} is the polarization due to muons stopping in the sample holder and windows, $\omega_L = 2\pi\nu_L$ is the muon Larmor frequency in radians per second, and ϕ is the phase. The frequencies and phases of the two components were common in the fits. P_{Bg} was determined from fitting the spectrum at 145 K, where the relaxation rate of the other signal is fastest, and fixed for the fits at all other temperatures. The two main structures with muons in a diamagnetic environment in PEO will be Mu^+ added to the oxygen atoms of PEO to give RO(Mu^+)R and MuH, which is formed by Mu abstraction. The contributions due to MuH have been ignored as it is only present in a very low concentration due to the slow abstraction rate compared with the time scale of the experiment and would only weakly interact with the polymer. The precession frequencies of paramagnetic states in a transverse field of 10 mT are too high to be resolved at ISIS. Contributions from the amorphous and crystalline regions cannot be distinguished as the muon is a local probe and not sensitive to long-range order.

The temperature dependence of the muon spin-spin relaxation rate ($1/T_2^\mu$) is shown in Fig. 5. $1/T_2^\mu$ increases with decreasing temperature and there is a distinct change in the temperature dependence at T_g, which suggests that different relaxation process dominate in the different temperature regimes. The motions cannot be described by the thermally activated behavior expected for a harmonic solid (i.e., $\ln\lambda \propto 1/T$). The temperature dependence of $1/T_2^\mu$ in 1-propanol, glycerol [25,26], and 2-adamantanone [27] were fit from the deep-glass phase up to the normal liquid with a simple square-root law based on the kinetic theory of the glass transition:

$$\frac{1}{T_2^\mu} = A\sqrt{\frac{|T - T_c|}{T_c}} + \xi(T), \quad T \leqslant T_c, \quad (6)$$

$$\frac{1}{T_2^\mu} = \xi(T) = a + b\frac{|T - T_c|}{T_c}, \quad T > T_c, \quad (7)$$

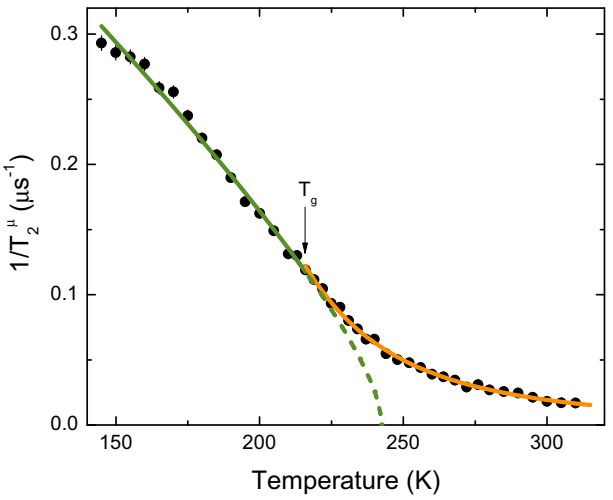

FIG. 5. Plot of $1/T_2^{\mu}$ versus temperature for PEO. The line for $T > T_g$ are fits to Eq. (11) and the line for $T < T_g$ are fits to Eq. (6). The dotted line is the extrapolation of Eq. (6) above T_g.

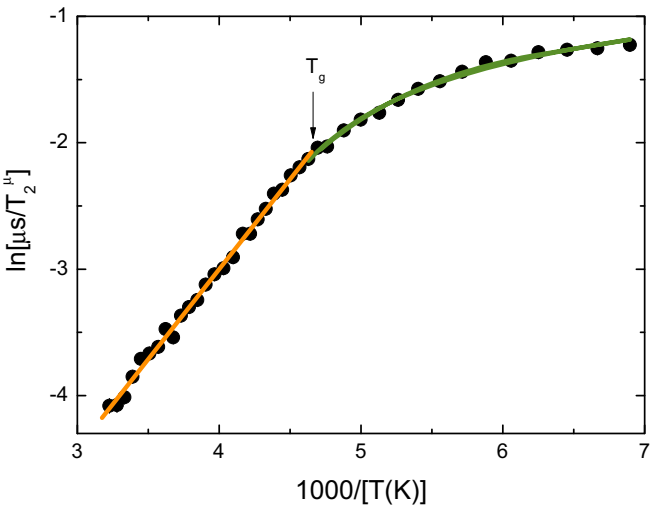

FIG. 6. Arrhenius plot of $\ln[\mu s/T_2^{\mu}]$ versus inverse temperature for PEO. The lines for $T > T_g$ are fits to Eq. (11) and the lines for $T < T_g$ are fits to Eq. (6).

where T_c is a critical temperature, which is above T_g; A is a global scaling constant; $\xi(T)$ is a background term determined from data measured above the transition; and a and b are parameters to account for the temperature dependence above T_c. These equations can be used to model the temperature dependence of $1/T_2^{\mu}$ in PEO below T_g but cannot explain the behavior over the entire range. The fitted parameters in PEO are $T_c = 242$ K, $A = 0.22\ \mu s^{-1}$, $a = 0$, and $b = 0.42\ \mu s^{-1}$. Our conclusion is that the spin relaxation below T_g is likely caused by Mu^+ vibrating within a cage formed by several PEO chains.

The spin relaxation above T_g is dominated by activated hopping of Mu^+. When the diffusion process is isotropic, the temperature and frequency dependence of relaxation rates can often be well described with the model introduced by Bloembergen, Purcell, and Pound (BPP) [28]:

$$\frac{1}{T_2} = \frac{K}{2}\left[3\tau + \frac{5\tau}{1+\omega_L^2\tau^2} + \frac{2\tau}{1+4\omega_L^2\tau^2}\right], \tag{8}$$

where K is a constant that depends on the relaxation mechanism. The BPP model predicts that $1/T_2$ increases with increasing τ, which occurs as the sample is cooled, and this is in agreement with observed behavior in PEO. The data above T_g could be fit assuming τ follows an Arrhenius temperature dependence:

$$\tau = \tau_0 \exp(E_A/k_B T), \tag{9}$$

where E_A is the activation energy, k_B is the Boltzmann constant, and τ_0 is the pre-exponential factor. The data over the entire temperature range could not be fit assuming a single E_A with the change in the temperature dependence at T_g being due to a change from the slow to fast fluctuation limits. The ZF-μSR measurements indicate that above T_g the PEO system is in the motional narrowed regime, i.e., $\omega_L^2\tau^2 \ll 1$. Under these conditions, Eq. (8) can be approximated as:

$$\frac{1}{T_2} = 5K\tau. \tag{10}$$

Combining the two previous equations gives:

$$\ln\left(\frac{\mu s}{T_2}\right) = \ln(5K\tau_0\,\mu s) + \left(\frac{E_A}{k_B}\right)T^{-1}. \tag{11}$$

An Arrhenius plot is shown in Fig. 6 and above T_g, $\ln(\mu s/T_2^{\mu})$ increases linearly with inverse temperature. The activation energy was determined from the slope and is 122 ± 1 meV. This is approximately half the barrier determined from low-frequency dielectric spectroscopy measurements. The difference in E_A arises from the muon being a local probe and is therefore less sensitive to macroscopic sample quality issues and long-range processes. We do not observe distinct signals from the crystalline and amorphous regions of PEO and so are observing an average of the dynamics in these different environments. The value of K is not known so the absolute value of τ cannot be calculated. τ changes by a factor of $\sim$2 going from 264 to 310 K, which is substantially less than the change in the τ of the acidic proton in deuterated PEO over a similar temperature interval [9]. The difference is most likely due to the high concentration of acidic protons in the NMR measurements, whereas the μSR measurements were performed in the infinite dilution limit. The light mass of the muon is only important at low temperatures where quantum tunneling is significant.

C. Radiolysis processes in PEO

The muon polarization is distributed into different fractions depending on the radiolysis processes that occur in a given material,

$$P_D + P_{Mu} + P_L + P_{Bg} = 1. \tag{12}$$

There is missing polarization due to Mu, P_{Mu}, whose precession frequencies are too high to be observed at ISIS in a magnetic field of 10 mT, and a lost fraction, P_L, due to muons that are rapidly depolarized during the radiolysis process. P_D changes substantially with temperature (Fig. 7).

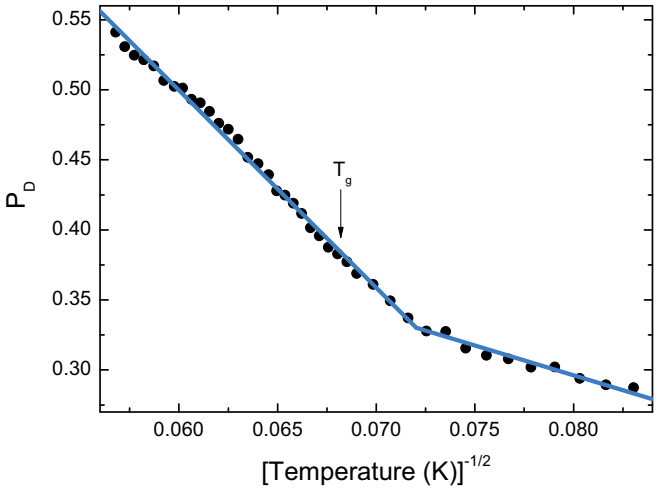

FIG. 7. Diamagnetic polarization, P_D, versus $T^{-1/2}$ in PEO. The solid lines are fits to Eq. (13).

The results of our measurements on PEO are very similar in many respects to the studies by Bermejo *et al.* of glasses of 1-propanol and glycerol where P_D increased with increasing temperature [25,26]. The smaller missing fraction at higher temperatures means that less Mu is being formed. Bermejo *et al.* proposed that Mu is formed by the reaction of a radiolytic electron with $ROHMu^+$, which is initially formed by Mu^+ addition to the alcohol. This is analogous to the dominant reaction in the radiolysis of water [29] and is favorable because of the opposite charges of the reacting species. Hopping of Mu^+ just regenerates $ROHMu^+$ while deprotonation of $ROHMu^+$ forms neutral ROMu (Fig. 8) and traps the muon in a diamagnetic state because the reaction of a solvated electron with an alcohol like ethanol is very slow ($\sim 1 \times 10^3$ $M^{-1}s^{-1}$ [30]) compared with the lifetime of the muon, which sets the time scale for the experiment. The lifetime of $ROHMu^+$ was assumed to be shorter at higher temperature, which would result in less Mu being formed. DFT calculations were performed on methanol to investigate the energetics of Mu^+ and H^+ hopping. The structures of the molecules shown in Fig. 8 with $R = CH_3$ were optimized and frequency calculations including anharmonic corrections were performed to determine the sum of the electronic and zero-point energies, E. These calculations accounted for the light mass of the muon and were used to calculate ΔE for Mu^+ and H^+ hopping. Mu^+ hopping regenerates the same species, so $\Delta E = 0$, while H^+ hopping leads to different isotopomers and is exothermic with $\Delta E = -22$ meV. This means that the muon will be rapidly trapped in the diamagnetic ROMu state. Regardless of the energetics, a similar process cannot occur in PEO because there is no proton attached to oxygen to hop and the $RO(Mu^+)R$ state cannot convert to a neutral state.

In order to account for the temperature dependence of A_D in PEO, it is necessary to take into account the heterogeneous distribution of the radiolytic electrons, which form in the spur caused by the muon, and their diffusion. Diffusion decreases the concentration of radiolytic electrons, ρ, near the $RO(Mu^+)R$ state, so less Mu is formed. We propose that the polarization of Mu is proportional to ρ. The situation is

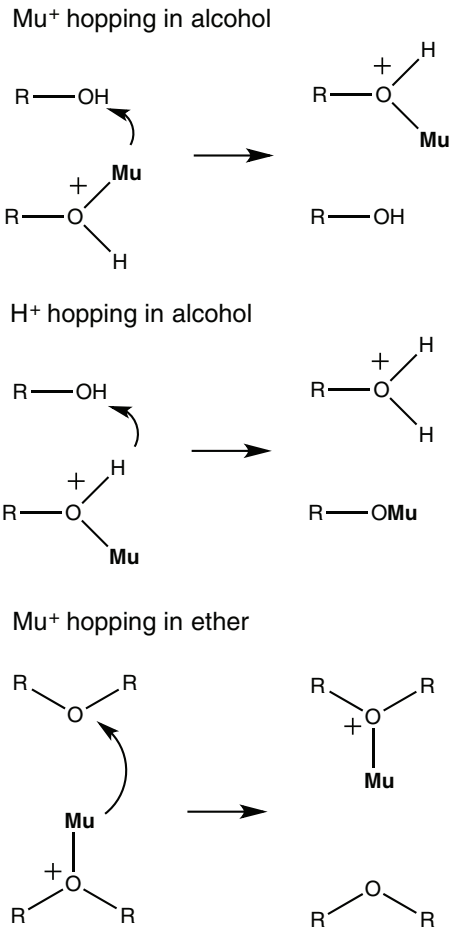

FIG. 8. Mu^+ and H^+ hopping in alcohols and ethers.

reminiscent of Brownian motion in that at $t = 0$ there is a concentration of particles at the origin, which we take to be the location of the $RO(Mu^+)R$ state, and they spread out with time. We use Einstein's expression for Brownian motion to account for the diffusion of the radiolytic electrons; ρ is proportional to $D^{-1/2}$, where D is the diffusion constant. D is proportional to T if the electron mobility is constant, and therefore our expectation is that

$$P_D = P' - cT^{-1/2}, \tag{13}$$

where $P' = 1 - P_L - P_{Bg}$ and c is a constant. The diamagnetic asymmetry was observed to decrease proportional to $T^{-1/2}$ (Fig. 7), which lends credence to our model. There is a change in the temperature dependence around ~195 K, which is ~20 K below T_g. The reason for the change in the temperature dependence occurring below T_g is not known. This mechanism could account for the temperature dependence of the diamagnetic fraction seen in the 1-propanol and glycerol glasses studied by Bermejo *et al.* [25,26].

IV. CONCLUSION

The microscopic dynamics of Mu^+, a light proton analog, have been studied in PEO with ZF-μSR and TF-μSR. The exponential relaxation in zero magnetic field, rather than Kubo-Toyabe relaxation, indicates that the system is in the fast

fluctuation limit. The relaxation of the muon spin polarization in a transverse field was found to be sensitive to the hopping rate of Mu^+, which has an Arrhenius temperature dependence above T_g with an activation barrier of 122 ± 1 meV. The diamagnetic fraction increased with increasing temperature and could be explained by the diffusion of radiolytic electrons away from the muon. This is the first organic material where μSR has been used to study the hopping of Mu^+ as a substitute for H^+. The success of these experiments shows that TF-μSR could be used to study the microscopic dynamics of Mu^+ in more commercially relevant proton-conducting membranes such as Nafion®.

ACKNOWLEDGMENTS

μSR measurements were performed under experiment RB1520031 at the ISIS pulsed neutron and muon facility.

[1] D. T. Hallinan Jr. and N. P. Balsara, Annu. Rev. Mater. Res. **43**, 503 (2013).
[2] W. Meyer, Adv. Mater **10**, 439 (1998).
[3] R. Pratap, B. Singh, and S. Chandra, J. Power Sources **161**, 702 (2006).
[4] B. Smitha, S. Sridhar, and A. Khan, J. Membr. Sci. **259**, 10 (2005).
[5] S. A. Hashmi, A. Kumar, K. K. Maurya, and S. Chandra, J. Phys. D: Appl. Phys. **23**, 1307 (1990).
[6] K. K. Maurya, N. Srivastava, S. A. Hashmi, and S. Chandra, J. Mater. Sci. **27**, 6357 (1992).
[7] G. A. Niklasson, Sol. Energ. Mat. Sol. Cells **92**, 1293 (2008).
[8] D. Q. M. Craig, J. M. Newton, and R. M. Hill, J. Mater. Sci. **28**, 405 (1993).
[9] P. Donoso, W. Gorecki, C. Berthier, F. Defendini, C. Poinsignon, and M. B. Armand, Solid State Ionics **28–30**, 969 (1988).
[10] J. Rault, J. Non-Cryst. Solids **271**, 177 (2000).
[11] V. G. Storchak and N. V. Prokof'ev, Rev. Mod. Phys. **70**, 929 (1998).
[12] A. Yaouanc and P. Dalmas de Réotier, *Muon Spin Rotation, Relaxation and Resonance: Applications to Condensed Matter* (Oxford University Press, Oxford, 2011).
[13] I. McKenzie, Annu. Rep. Prog. Chem., Sect. C: Phys. Chem. **109**, 65 (2013).
[14] N. J. Clayden and S. P. Cottrell, Phys. Chem. Chem. Phys. **8**, 3094 (2006).
[15] G. M. Luke, J. H. Brewer, S. R. Kreitzman, D. R. Noakes, M. Celio, R. Kadono, and E. J. Ansaldo, Phys. Rev. B **43**, 3284 (1991).
[16] T. Lancaster, F. L. Pratt, S. J. Blundell, I. McKenzie, and H. E. Assender, J. Phys.: Condens. Matter **21**, 346004 (2009).
[17] I. McKenzie, Z. Salman, S. R. Giblin, Y. Y. Han, G. W. Leach, E. Morenzoni, T. Prokscha, and A. Suter, Phys. Rev. E **89**, 022605 (2014).
[18] J. Mattsson, J. A. Forrest, A. Krozer, U. Södervall, A. Wennerberg, and L. M. Torell, Electrochim. Acta **45**, 1453 (2000).
[19] S. R. Giblin, S. P. Cottrell, P. J. C. King, S. Tomlinson, S. J. S. Jago, L. J. Randall, M. J. Roberts, J. Norris, S. Howarth, Q. B. Mutamba, N. J. Rhodes, and F. A. Akeroyd, Nucl. Instrum. Methods Phys. Res., Sect. A **751**, 70 (2014).
[20] M. J. Frisch, G. W. Trucks, H. B. Schlegel, G. E. Scuseria, M. A. Robb, J. R. Cheeseman, G. Scalmani, V. Barone, G. A. Petersson, H. Nakatsuji, X. Li, M. Caricato, A. Marenich, J. Bloino, B. G. Janesko, R. Gomperts, B. Mennucci, H. P. Hratchian, J. V. Ortiz, A. F. Izmaylov, J. L. Sonnenberg, D. Williams-Young, F. Ding, F. Lipparini, F. Egidi, J. Goings, B. Peng, A. Petrone, T. Henderson, D. Ranasinghe, V. G. Zakrzewski, J. Gao, N. Rega, G. Zheng, W. Liang, M. Hada, M. Ehara, K. Toyota, R. Fukuda, J. Hasegawa, M. Ishida, T. Nakajima, Y. Honda, O. Kitao, H. Nakai, T. Vreven, K. Throssell, J. A. Montgomery, Jr., J. E. Peralta, F. Ogliaro, M. Bearpark, J. J. Heyd, E. Brothers, K. N. Kudin, V. N. Staroverov, T. Keith, R. Kobayashi, J. Normand, K. Raghavachari, A. Rendell, J. C. Burant, S. S. Iyengar, J. Tomasi, M. Cossi, J. M. Millam, M. Klene, C. Adamo, R. Cammi, J. W. Ochterski, R. L. Martin, K. Morokuma, O. Farkas, J. B. Foresman, and D. J. Fox, *Gaussian 09 Revision D.01* (Gaussian, Inc., Wallingford CT, 2016).
[21] J. Sugiyama, K. Mukai, Y. Ikedo, H. Nozaki, M. Månsson, and I. Watanabe, Phys. Rev. Lett. **103**, 147601 (2009).
[22] J. Sugiyama, H. Nozaki, M. Harada, K. Kamazawa, O. Ofer, M. Månsson, J. H. Brewer, E. J. Ansaldo, K. H. Chow, Y. Ikedo, Y. Miyake, K. Ohishi, I. Watanabe, G. Kobayashi, and R. Kanno, Phys. Rev. B **84**, 054430 (2011).
[23] J. Sugiyama, H. Nozaki, I. Umegaki, K. Mukai, K. Miwa, S. Shiraki, T. Hitosugi, A. Suter, T. Prokscha, Z. Salman, J. S. Lord, and M. Månsson, Phys. Rev. B **92**, 014417 (2015).
[24] J. H. van Vleck, Phys. Rev. **74**, 1168 (1948).
[25] F. J. Bermejo, I. Bustinduy, M. A. González, S. H. Chong, C. Cabrillo, and S. F. J. Cox, Phys. Rev. B **70**, 214202 (2004).
[26] F. J. Bermejo, I. Bustinduy, S. F. J. Cox, J. S. Lord, C. Cabrillo, and M. A. Gonzalez, J. Phys.: Condens. Matter **18**, 2871 (2006).
[27] M. Romanini, J. L. Tamarit, L. C. Pardo, F. J. Bermejo, R. Fernandez-Perea, and F. L. Pratt, J. Phys.: Condens. Matter **29**, 085405 (2017).
[28] N. Bloembergen, E. M. Purcell, and R. V. Pound, Phys. Rev. **73**, 679 (1948).
[29] P. W. Percival, K. M. Adamson-Sharpe, J.-C. Brodovitch, S.-K. Leung, and K. E. Newman, Chem. Phys. **95**, 321 (1985).
[30] H.-R. Park and N. Getoff, Z. Naturforsch., A: Phys. Sci. **47A**, 985 (1992).